Penerbit Akademia Baru

Journal of Advanced Research in Fluid Mechanics and Thermal Sciences

Journal homepage: www.akademiabaru.com/arfmts.html
ISSN: 2289-7879

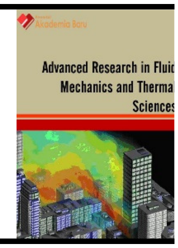

Open Access

Analysis of Stagnation Point flow of an Incompressible Viscous Fluid between Porous Plates with Velocity Slip

Ashwini Bhat[1,*], Nagaraj N Katagi[1]

[1] Department of Mathematics, Manipal Institute of Technology, Manipal Academy of Higher Education, Udupi Karkala Road, Manipal, Karnataka-576104, India

ARTICLE INFO

Article history:
Received 8 April 2018
Received in revised form 12 June 2018
Accepted 1 July 2018
Available online 12 August 2018

ABSTRACT

The present study investigates the effects of slip velocity on the stagnation point of an incompressible viscous fluid between porous plates. The appropriate slip boundary conditions have been introduced in place of no-slip condition. The governing equations of motion is solved by Homotopy analysis and Computer extended series method. Padé approximants are further used to increase the domain and rate of convergence of the series so generated. The above methods admits a desired accuracy whose validity increases up to a sufficiently large values of R, Reynolds number with different slip coefficients. The approximate analytical results have been verified to be very accurate when compared with the previous solutions observed by Chapman in the absence of slip coefficient.

Keywords:
Stagnation point flow, slip velocity, computer extended series, homotopy analysis method, Domb-Sykes plot.

1. Introduction

The study of flow between the porous or non-porous disk has significant importance due to its applications in both scientific and industry. These types of flows have applications in bio-mechanics, semiconductor manufacturing process with rotating wafers, hydrodynamical machines, etc. Hiemenz [1] was the first researcher to propose the basic two dimensional stagnation flow towards plate. Later, this study was extended to three dimensional case Howarth [2] and Davey[3]. Axisymmetric stagnation flow on a cylinder was solved by Wang [4]. Many researchers have investigated the problem on fluid flow between porous plates/ disks with suction or blowing[5, 6-10]. Rasmussen[11] numerically analysed the problem of flow between two porous co-axial disks. Chapman and Bauer[12] presented the asymptotic and numerical solution for stagnation point viscous flow between porous plates with uniform blowing. Later, the problem of steady stagnation point flow of an incompressible micro-polar fluid between two porous disks with uniform blowing was analyzed by Agarwal and Dhanpal [13]. They have used shooting techniques for numerical solutions. Elcrat [14] obtained the theorem of existence and uniqueness for non-rotational fluid motion between fixed

* *Corresponding author.*
E-mail address: Ashwini.bhat@manipal.edu (Ashwini Bhat)

porous disks with arbitrary suction or blowing. Bujurke *et al*., [15] discussed the solution of viscous flow between two parallel porous plates by computer extended series analysis followed by Euler transformation to increase the validity of series. A brief review of works on stagnation point flow can be found in paper by Wang [16,17]. Mahapatra and Gupta [18] studied the laminar steady stagnation-point flow of a viscoelastic fluid over a stretching surface; they studied flow when the stretching velocity of the surface is more (less) than the free stream velocity. Following this work, an extensive work has been carried out by many experts on the stagnation-point flow of viscoelastic fluid past a stretching surface. In all the above analysis of flow with porous boundaries, a zero slip condition was assumed, which characterizes flow with the solid boundary walls. Howeve, the effect of slip was not considered by them. Beavers and Joseph [19] proved the existence of slip velocity at a porous surface through theoretical explanations and experimental observations. The historical background to Beavers - Joseph conditions at the interface of porous media and clear fluid were reported by Neild [20]. Ashwini *et al*., [21,22] have implemented successfully these Beavers - Joseph conditions in the analysis of flow in channels and pipes.

It is clear from the literature that no attempts have been made to analyse the influence of slip velocity on the stagnation point flow of an incompressible viscous fluid between porous plates. The current analysis has developed a model for the same by taking into consideration the velocity slip effects and filled this gap. The obtained solutions are in well agreement with that of Chapman and Bauer**Error! Reference source not found.** for smaller and large values of Reynolds number when slip effect is zero. The resulting governing equations with slip boundary conditions are solved by two novel semi-analytical techniques for different values of slip coefficient at different Reynolds number. The influence of slip coefficient on pressure gradient, variations in dimensionless axial velocity, dimensionless axial velocity derivative in the presence of velocity slip have been analysed.

2. Mathematical Formulation

Consider a steady, axially symmetric, laminar flow of a viscous incompressible fluid between two parallel porous disks separated by a distance $2L$ (Figure 1). The fluid with uniform velocity having magnitude V is injected through both porous plates, continuously which flows radially towards middle plane $Z=0$.

Under the assumed conditions, the relevent continuity and momentum equations which governs the flow field and pressure distribution are [9],

$$\frac{1}{r}\frac{\partial}{\partial r}(rv_r)+\frac{\partial}{\partial z}v_z=0 \tag{1}$$

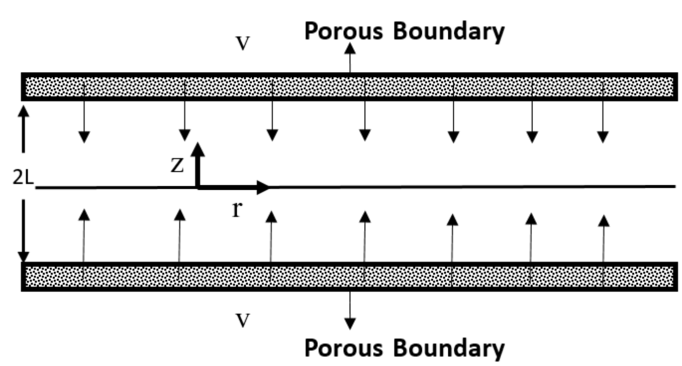

Fig. 1. Geometry of axi-symmetric flow between porous plates with uniform injection velocities

r-momentum and z-momentum equations.

$$\rho(v_r\frac{\partial v_r}{\partial r}+v_z\frac{\partial v_r}{\partial z})=-\frac{\partial p}{\partial r}+\mu(\frac{\partial}{\partial r}(\frac{1}{r}\frac{\partial(rv_r)}{\partial r})+\frac{\partial^2 v_r}{\partial z^2}) \tag{1}$$

$$\rho(v_r\frac{\partial v_z}{\partial r}+v_z\frac{\partial v_z}{\partial z})=-\frac{\partial p}{\partial z}+\mu(\frac{1}{r}\frac{\partial}{\partial r}(r\frac{\partial v_z}{\partial r})+\frac{\partial^2 v_z}{\partial z^2})-\rho g \tag{2}$$

It is assumed that $v_\theta=0$.
The boundary conditions are,
$v_z = -V$ at $z = L$ (3)
$v_r = v_{slip}$ at $z = L$ (4)
$v_z = 0$ at $z = 0$ (5)
$\frac{\partial v_r}{\partial z} = 0$ at $z = 0$ (6)
and $P=P_0$ at $r = 0, z = 0$ (7)

The boundary conditions (6) and (7) are due to planar symmetry, that is we consider only upper half of the flow field and Equation (4) is the slip boundary condition by Beavers and Joseph [16]. The slip velocity at porous surface is being proportional to shear rate at the porous boundary, we have $v_r = v_{slip} = -\phi\frac{\partial v_r}{\partial \xi}$, where $\phi = \frac{\sqrt{k}}{\alpha L}$ is the slip coefficient.

Because of the symmetrical geometrical properties and uniform boundary conditions, it allows to assume,
$v_r = r\varphi(z)$ (8)

So that, $\frac{\partial v_z}{\partial z} = -2\phi(z)$ (9)

Substituting (8) and (9) into (1) and (2) concludes that the quantity, $[-\frac{\partial P}{\partial r}/r]$ is a constant. Equation (1) becomes,

$$\frac{\rho}{4}(\frac{dv_z}{dz})^2-\rho\frac{v_z}{2}(\frac{d^2v_z}{dz^2})+\frac{\mu}{2}(\frac{d^3v_z}{dz^3})=[-\frac{\partial P}{\partial r}/r] \tag{11}$$

Now, with dimensionless quantities defined as,

$$\xi=\frac{z}{L},\ \theta=\frac{v_z}{V},\ Re=\frac{LV\rho}{\mu}\ \text{and}\ D_p=[-4\frac{\partial P}{\partial r}\frac{L^2}{\rho r V^2}] \tag{10}$$

Equation **Error! Reference source not found.** reduces to

$$\frac{2}{Re}\theta'''(\xi)-2\theta(\xi)\theta''(\xi)+(\theta'(\xi))^2 = D_p \tag{11}$$

or

$$\theta''''(\xi) = Re\ \theta(\xi)\theta'''(\xi) \tag{12}$$

The boundary conditions (4)-(7) reduces to,

$\theta = -1$ at $\xi = 1$ (13)
$\theta = 0$ at $\xi = 0$ (14)
$\theta'' = 0$ at $\xi = 0$ (15)

and $\theta' = -\varphi\theta''$ at $\xi = 1$ where $\varphi = -\frac{\sqrt{k}}{\alpha L}$, slip coefficient. (16)

Also, from (2), (7) and (10) the solution for pressure gradient can be rewritten as,

$$P = P_0 - \frac{\mu V}{L}\int_0^{\xi}[R\theta\theta' - \theta'']d\xi - \frac{\rho V^2 D_p r^2}{8L^2}. \tag{17}$$

From (8) and (9) the radial component of velocity is given by,

$$v_r = \frac{-V}{2L} r\theta'(\xi) \tag{18}$$

Thus Equation (12) along with boundary conditions (13)-(16) describes the entire flow situation and expressions for $\theta(\xi, R)$, $D_p(R)$ provides solution to the problem. Solution of Equation (12) is usually solved by direct integration which frequently involves more than one integration process because of two point nature of boundary conditions. Thus the use of proposed series method provides an attractive alternative approach. Also, the terms in the series method are capable of providing results to any desired accuracy.

3. Method of Solution

3.1 Series Solution Method

We seek the solution of equation (12) for small values of R can be expressed in the form of power series as,

$$\theta(\xi) = \theta_0(\xi) + \sum_{n=1}^{\infty} R^n \theta_n(\xi) \tag{19}$$

substituting equation (19) into equation (12) and comparing like powers of R on both sides, we get,

$$\theta_n'''' = \sum_{r=0}^{n-1} \theta_{n-1-r}'''' \theta_r''', n = 1,2,3,\ldots \tag{20}$$

the boundary conditions are,

$$\theta_n(0) = 0, \theta_{n''}(0) = 0, \quad \forall n \geq 0 \tag{21}$$

$$\theta_0(1) = -1, \theta_n(1) = 0, \ \forall n \geq 1 \tag{22}$$

$$\theta_{n'}(1) = -\varphi \theta_{n''}(1) \ \ \forall n \geq 0 \tag{23}$$

The solution of above system of equations up to term in R are,

$$\begin{aligned}
\theta_0(\xi) &= \frac{\xi^3 - 6\xi\phi - 3\xi}{2(3\phi+1)} \\
\theta_1(\xi) &= \frac{0.00178571\left(3\xi^7\phi + \xi^7 - 126\xi^5\phi^2 - 105\xi^5\phi - 21\xi^5 + 420\xi^3\phi^2 + 273\xi^3\phi + 39\xi^3 - 294\xi\phi^2 - 171\xi\phi - 19\xi\right)}{(3\phi+1)^3}
\end{aligned} \tag{24}$$

The solution for $\phi = 0$ is given by Chapman and Bauer [9].

Computer extended perturbation solution:

As the series (20) is slowly converging, it is not possible to analyze the problem accurately with just two terms [23,24]. We need sufficiently large number of universal polynomial coefficients which reveal the true nature of the solution represented by series (19) [25,26]. Manually evaluating the coefficients beyond second order terms is very difficult as one proceeds to higher approximations the algebra becomes cumbersome. Towards this goal, we proposed recurrence relations along with Mathematica, which efficiently generates higher order terms of the series.

The axial velocity component is directly obtained as $\theta(\xi)$ and dimensionless axial velocity derivative is,

$$\theta'(\xi) = \theta_{0'}(\xi) + \sum_{n=1}^{\infty} R^n \theta_{n'}(\xi) = \sum_{n=0}^{\infty} R^n a_n \tag{25}$$

The dimensionless pressure gradient D_p is represented by the series,

$$D_p = \frac{2}{R}\theta'''(1) + 2\theta''(1) \tag{26}$$

Coefficients of the series (19) representing $\theta(\xi)$ and pressure gradient (26) are decreasing in magnitude and have no fixed sign pattern. Domb-Sykes plot [27] is drawn to find the nature of nearest singularities which restricts convergence of the series.

3.2 Homotopy Analysis Method

To compare the solution obtained by extended series method, we also solve the governing equations with boundary conditions by another useful semi analytical technique called Homotopy analysis method (HAM). As HAM does not depend on a small parameter like other series methods and allows to transfer a non-linear problem into an infinite number of linear sub-problems, along with Padé sum it guarantees convergence of the solution in any case.

Zeroth-order deformation problem:

We seek solution of Equation (12) by using HAM and choose the base function to express $\theta(\xi)$ [28,29]. The initial guess which satisfies the boundary conditions is

$$\theta_0(\xi) = \frac{\xi^3}{2(3\phi+1)} - \frac{3\xi\phi}{3\phi+1} - \frac{3\xi}{2(3\phi+1)} \tag{27}$$

and auxiliary linear operator is given by,

$$L[\theta] = \theta'''' \tag{28}$$

The above linear operator which satisfies the following property,

$$L[C_1\frac{\xi^3}{6} + C_2\frac{\xi^2}{2} + C_3\xi + C_4] = 0$$

where C_1, C_2, C_3 and C_4 are constants to be determined. If $q \in [0,1]$ then the zeroth order deformation problem can be constructed as,

$$(1-q)L[\theta(n,q) - \theta_0(\xi)] = qhH(\xi)N[\theta(\xi,q)] \tag{29}$$

with relevant boundary conditions,

$$\begin{aligned} \theta(0,q) &= 0 \\ \theta(1,q) &= 1 \\ \theta'(1,q) &= -\phi\theta''(1,q) \\ \theta''(0,q) &= 0 \end{aligned} \tag{30}$$

where $0 \le q \le 1$ is an embedding parameter, h and H are non-zero auxiliary parameter and auxiliary function respectively. Further, N is a non-linear differential operator and is defined as,

$$N[\theta(\xi,q)] = \frac{\partial^4\theta(\xi,q)}{\partial\xi^4} - R\theta(\xi,q)\frac{\partial^3\theta(\xi,q)}{\partial\xi^2} \tag{31}$$

For $q = 0$ and $q = 1$, Equation (29) has solution,

$$\begin{aligned} \theta(\xi,0) &= \theta_0(\xi) \\ \theta(\xi,1) &= \theta(\xi) \end{aligned} \tag{32}$$

As q varies from 0 to 1, $\theta(\xi,q)$ varies from initial guess $\theta_0(\xi)$ to exact solution $\theta(\xi)$ By Taylor's theorem, Equation (32) can be expressed as

$$\theta(\xi,q)=\theta_0(\xi)+\sum_{m=1}^{\infty}\theta_m(\xi)q^m \tag{33}$$

where, $\theta_m(\xi)=\frac{1}{m!}\frac{\partial^m\theta}{\partial q^m}|_{q=0}$. Convergence of the above series (33) depends on the convergence control parameter h, which is chosen in such a way that (33) is convergent at $q=1$. Then we have,

$$\theta(\xi)=\theta_0(\xi)+\sum_{m=1}^{\infty}\theta_m(\xi) \tag{34}$$

mth-order deformation problem:

Differentiating the zeroth order deformation problem equation-(29) 'm' times with respect to q and lastly setting $q=0$. The resulting m^{th} order deformation problem becomes,

$$L[\theta_m(\xi)-\chi_m\theta_{m-1}(\xi)]=hH(\xi)\Re_m(\xi) \tag{35}$$

and the homogeneous boundary conditions are,

$$\theta_m(0)=0,\ \theta_m(1)=0,\ \theta_{m'}(1)=-\phi\theta_{m''}(1),\theta_{m''}(0)=0 \tag{36}$$

where

$$\Re_m(\xi)=\theta_{m-1}{}'''-R\sum_{n=0}^{m-1}\theta_n\theta_{m-n-1}{}'' \tag{37}$$

and

$$\chi_m=\begin{cases}0, & m\le 1\\ 1, & m>1\end{cases} \tag{38}$$

We systematically utilized Mathematical software, Mathematica to obtain the solution for system of linear equations (35) with appropriate homogeneous boundary conditions (36). The solutions up to second order approximations are shown is Eq. (41).

Convergence of HAM:

The proposed series (34) contains the auxiliary parameter h which influences the convergence region and rate of approximations for the HAM solutions. This parameter is known as convergence control parameter. To ensure this series converges, we need to choose a suitable value for h. To obtain the permissible ranges of the parameter h, h-curves are plotted (Fig.6). Figure 6 shows $h-$ curve for the series D_p for corresponding values of R and slip coefficient ϕ at 10th order approximation.

$$
\begin{aligned}
\theta_1(\xi) &= \frac{1}{560(3\phi+1)^3}(-3h\xi^7R\phi - h\xi^7R + 126h\xi^5R\phi^2 + 105h\xi^5r\phi + 21h\xi^5R - 420h\xi^3R\phi^2 - 273h\xi^3R\phi \\
&\quad -39h\xi^3R + 294h\xi R\phi^2 + 171h\xi R\phi + 19h\xi R) \\
\theta_2(\xi) &= \frac{1}{2587200(3\phi+1)^5}(567h^2\xi^{11}R^2\phi^2 + 378h^2\xi^{11}R^2\phi + 63h^2\xi^{11}R^2 - 27720h^2\xi^9R^2\phi^3 - 32340h^2\xi^9R^2\phi^2 \\
&\quad -12320h^2\xi^9R^2\phi - 1540h^2\xi^9R^2 + 374220h^2\xi^7R^2\phi^4 + 665280h^2\xi^7R^2\phi^3 + 425502h^2\xi^7R^2\phi^2 \\
&\quad +116820h^2\xi^7R^2\phi + 11682h^2\xi^7R^2 - 873180h^2\xi^5R^2\phi^4 - 1397088h^2\xi^5R^2\phi^3 - 792792h^2\xi^5R^2\phi^2 \\
&\quad -188496h^2\xi^5R^2\phi - 15708h^2\xi^5R^2 + 291060h^2\xi^3R^2\phi^4 + 443520h^2\xi^3R^2\phi^3 + 197043h^2\xi^3R^2\phi^2 \\
&\quad +31010h^2\xi^3R^2\phi + 2215h^2\xi^3R^2 + 207900h^2\xi R^2\phi^4 + 316008h^2\xi R^2\phi^3 + 202020h^2\xi R^2\phi^2 + 52608h^2\xi R^2\phi \\
&\quad +3288h^2\xi R^2 - 124740h^2\xi^7R\phi^3 - 124740h^2\xi^7R\phi^2 - 41580h^2\xi^7R\phi - 4620h^2\xi^7R + 5239080h^2\xi^5R\phi^4 \\
&\quad +7858620h^2\xi^5R\phi^3 + 4365900h^2\xi^5R\phi^2 + 1067220h^2\xi^5R\phi + 97020h^2\xi^5R - 17463600h^2\xi^3R\phi^4 \\
&\quad -22993740h^2\xi^3R\phi^3 - 11129580h^2\xi^3R\phi^2 - 2342340h^2\xi^3R\phi - 180180h^2\xi^3R + 12224520h^2\xi R\phi^4 \\
&\quad +15259860h^2\xi R\phi^3 + 6888420h^2\xi R\phi^2 + 1316700h^2\xi R\phi + 87780h^2\xi R - 124740h\xi^7R\phi^3 - 124740h\xi^7R\phi^2 \\
&\quad -41580h\xi^7R\phi - 4620h\xi^7R + 5239080h\xi^5R\phi^4 + 7858620h\xi^5R\phi^3 + 4365900h\xi^5R\phi^2 + 1067220h\xi^5R\phi \\
&\quad +97020h\xi^5R - 17463600h\xi^3R\phi^4 - 22993740h\xi^3R\phi^3 - 11129580h\xi^3R\phi^2 - 2342340h\xi^3R\phi - 180180h\xi^3R \\
&\quad +12224520h\xi R\phi^4 + 15259860h\xi R\phi^3 + 6888420h\xi R\phi^2 + 1316700h\xi R\phi + 87780h\xi R)
\end{aligned}
\tag{39}
$$

4. Results

The equation of motion for steady stagnation point flow between two parallel plates is governed by nonlinear differential equation (12) together with boundary conditions (13)-(16) are solved by computer extended series method and Homotopy Analysis Method. We study the effect of slip coefficient on velocity profiles and pressure gradient at different Reynolds number. The results for velocity profiles and pressure gradient have been presented through figures and tables.

The proposed series expansion scheme using recurrence relation and Mathematica software we generate large number $(n = 30)$ of universal polynomial functions $\theta_n(\xi)$ for different slip coefficients ϕ. The series representing velocity profiles $\theta(\xi)$, $\theta'(\xi)$ and pressure gradient D_p are analyzed using Padé approximants for larger Reynolds number *R* for different slip coefficients. Domb-Sykes plot given in Figure 2 shows the singularity restricting convergence of the series representing velocity profiles, which gives the nature and location of nearest singularity. After extrapolation, using rational approximation yields the radius of convergence of series (25) to be 9.07441, 9.10747 and 9.37207 for $\varphi = 0, 0.1$ and 0.5 respectively.

The influence of slip coefficient on the velocity profiles are shown in Figure 3 which are found to be identical with HAM curves. It shows that velocity profiles are decreasing with increasing value of R. It is also observed that the shape of axial velocity profiles does not depend very strongly on Reynolds number.

Figure 4 shows the variation of axial velocity derivative profiles for different values of Reynolds number *R*. It is noted that larger values of Reynolds number *R* results in linear profiles. Influence of slip coefficient ϕ on pressure gradient is explained by Figure 5. It is seen that pressure gradient, D_p decreases with the influence of ϕ and attains a constant value D_p =4, 3.55 and 3.32 for ϕ = 0, 0.1 and 0.5 respectively. To check validity of the methods, results were compared for $\phi = 0$ with that of Chapman and Bauer **Error! Reference source not found.** are given in Table 1. The agreement with earlier findings is an excellent lending support to the methods proposed.

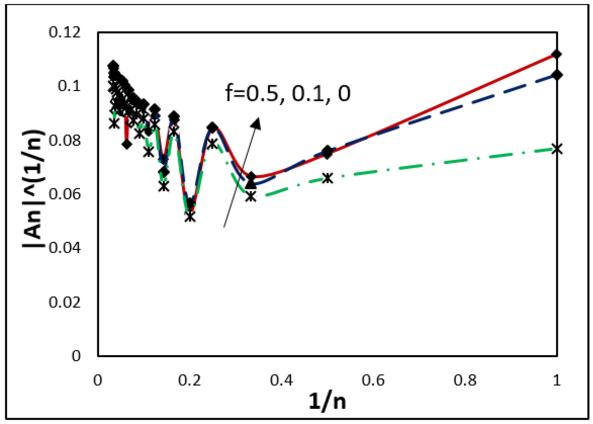

Fig. 2. Domb-Syke plot for velocity profiles

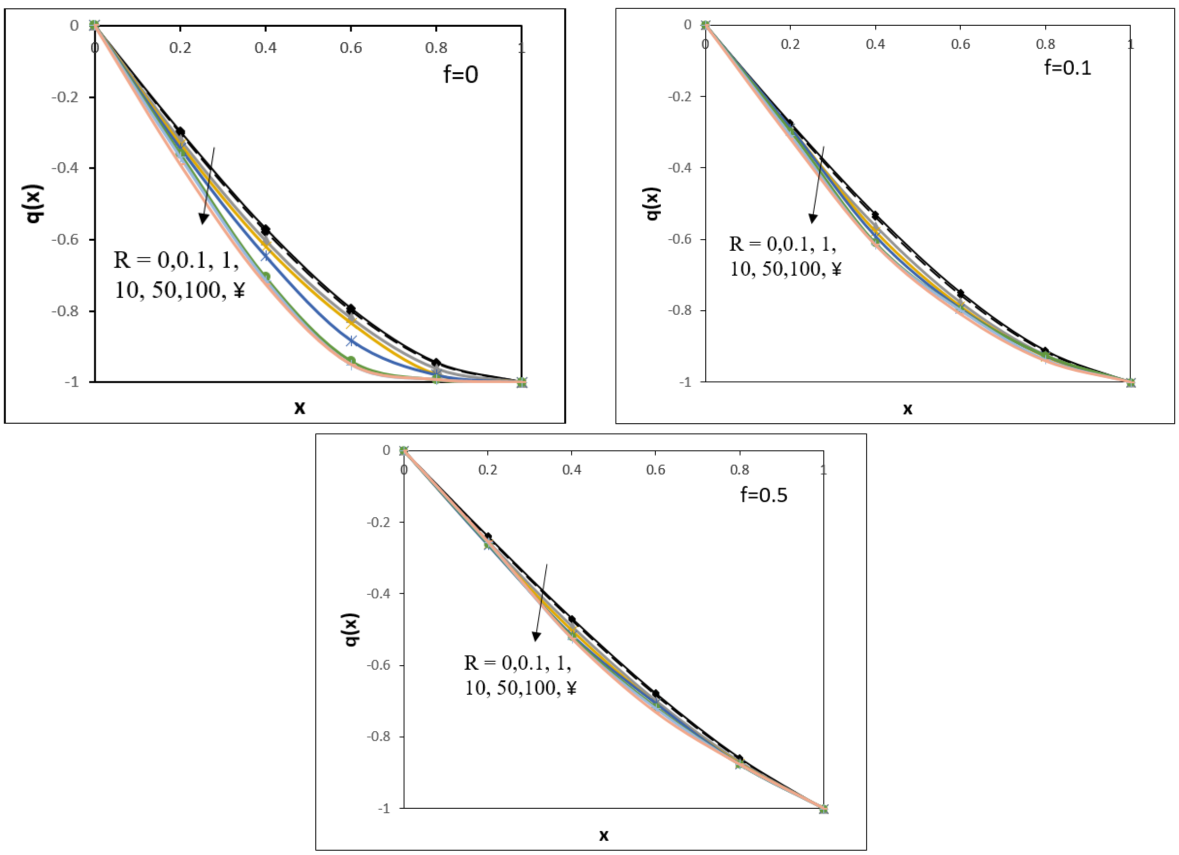

Fig. 3. Variation in dimensionless axial velocity for different Reynolds number R

Journal of Advanced Research in Fluid Mechanics and Thermal Sciences
Volume 48, Issue 1 (2018) 40-52

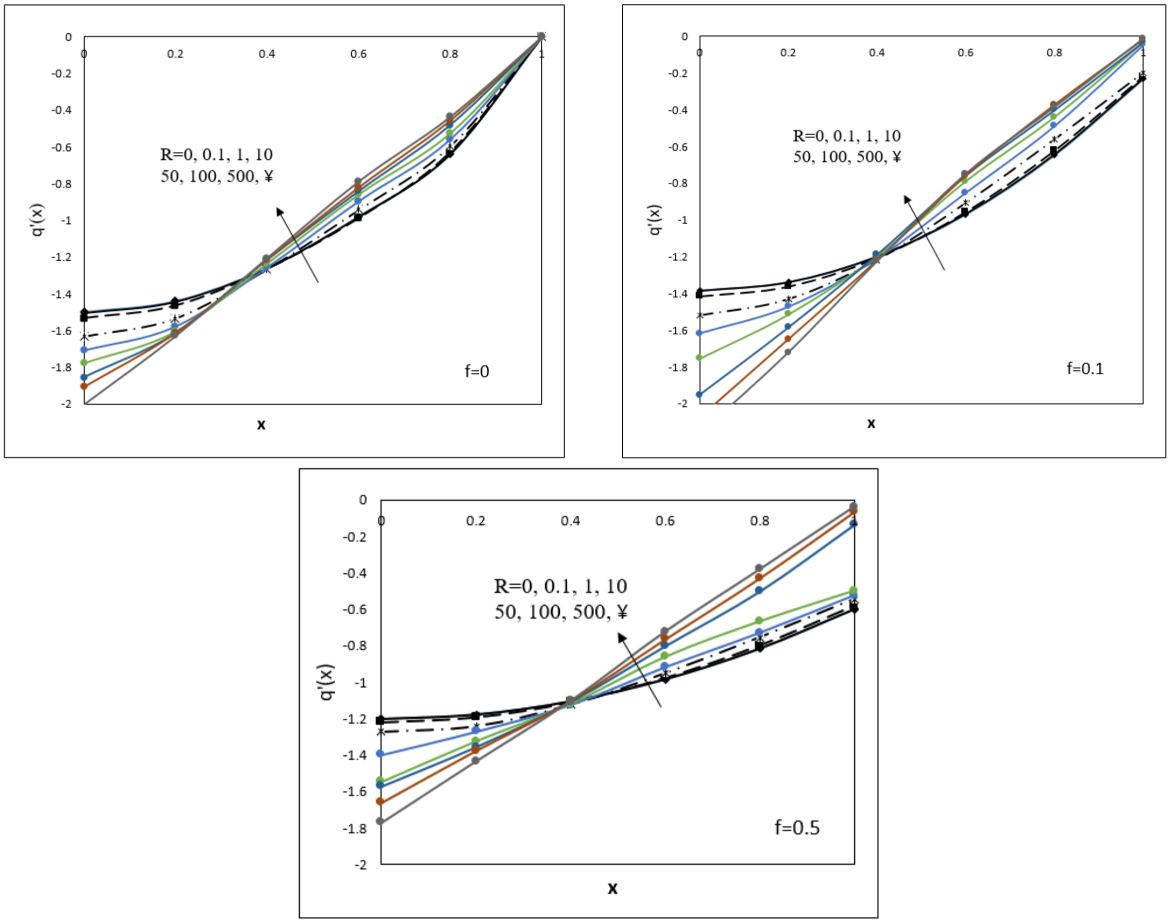

Fig. 4. Variation in dimensionless axial velocity derivative for different Reynolds number

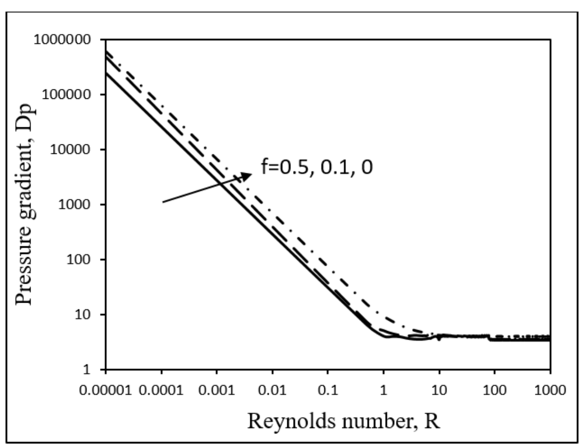

Fig. 5. Dimensionless pressure gradient as a function of Reynolds number for different slip coefficient $\phi = 0,0.1,0.5$

To compare and prove efficiency of the results obtained by Computer extended Series method, the problem is additionally analyzed by homotopy analysis method (HAM) alongside Padé sum to accelerate convergence of the series. We plot h-curves to discover the convergence range and furthermore the rate of approximations for the series representing $\theta'(0)$ and D_p when $R = 0.1,\ \phi = 0$ respectively from 10^{th} order HAM approximations. The range for admissible values of h for different values of R and ϕ is different. From the figures 6 and 7 it is observed that series representing $\theta'(0)$ and D_p are convergent when $-2.2 \leq h \leq -0.1$ and $-2.8 \leq h \leq -0.7$ respectively.

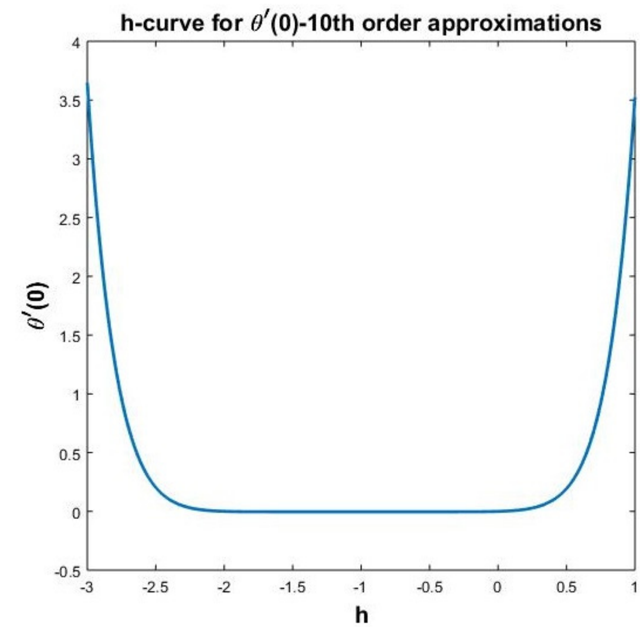

Fig. 6. h-curves for $\theta'(0)$ -10th order approximations

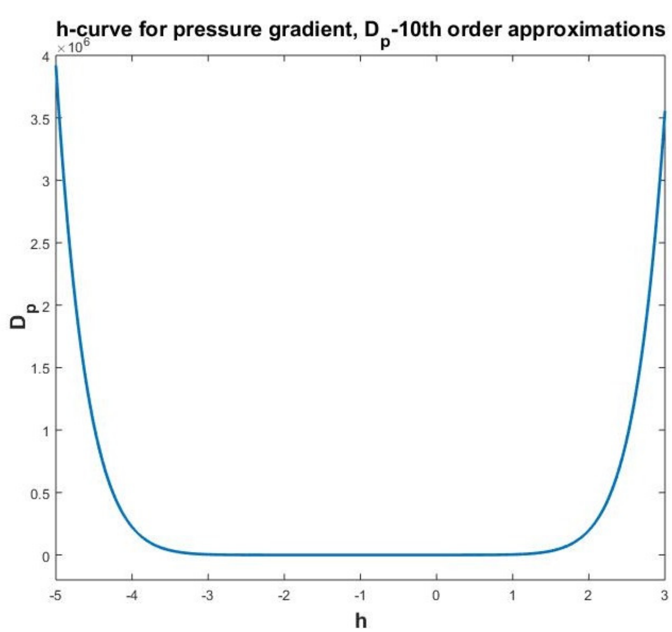

Fig. 7. h-curves for pressure gradient, D_p -10th order approximations

5. Conclusions

In this article, we have examined the steady stagnation point flow between two permeable plates by Computer Extended Series method (CES) and Homotopy Analysis Method (HAM). The impact of non-zero tangential slip velocity on velocity field and pressure gradient are analysed. The validity of series solution is extended to a large values of Reynolds number by utilizing analytic continuation. The examination affirms that the proposed methods converges to the solution for very large values of Reynolds number as compared to the earlier findings when slip coefficient is reduced to zero.

References

[1] Hiemenz, Karl. "Die Grenzschicht an einem in den gleichformigen Flussigkeitsstrom eingetauchten geraden Kreiszylinder." *Dinglers Polytech. J.* 326 (1911): 321-324.

[2] Howarth, L. "CXLIV. The boundary layer in three dimensional flow.—Part II. The flow near a stagnation point." *The London, Edinburgh, and Dublin Philosophical Magazine and Journal of Science* 42, no. 335 (1951): 1433-1440.

[3] Davey, A. "Boundary-layer flow at a saddle point of attachment." *Journal of Fluid Mechanics* 10, no. 4 (1961): 593-610.

[4] Wang, Chang-Yi. "Axisymmetric stagnation flow on a cylinder." *Quarterly of Applied Mathematics* 32, no. 2 (1974): 207-213.

[5] Berman, Abraham S. "Laminar flow in channels with porous walls." *Journal of Applied physics* 24, no. 9 (1953): 1232-1235.

[6] Sellars, John R. "Laminar flow in channels with porous walls at high suction Reynolds numbers." *Journal of Applied Physics* 26, no. 4 (1955): 489-490.

[7] Yuan, S. W. "Further investigation of laminar flow in channels with porous walls." *Journal of Applied Physics* 27, no. 3 (1956): 267-269.

[8] Mahmud, K. R., M. M. Rhaman, and A. K. Al Azad. "Numerical Simulation and Analysis of Incompressible Newtonian Fluid Flows using FreeFem+." *Journal of Advanced Research in Fluid Mechanics and Thermal Sciences* 26: 1-19.

[9] Ahmed. L. Abdullah, and Fuat Yilmaz. "Computational Analysis of Heat Transfer Enhancement in a Circular Tube Fitted with Different Inserts." *Journal of Advanced research in fluid mechanics and thermal sciences*. 40(2017): 59-69.

[10] Soo Weng Beng, and Wan Mohd. Arif Aziz Japar. "Numerical Analysis of Heat and Fluid Flow in Microchannel Heat Sink with Triangular Cavities". *Journal of Advanced research in fluid mechanics and thermal sciences*. 34(2017): 01-08.

[11] Rasmussen, Henning. "Steady viscous flow between two porous disks." *Zeitschrift für angewandte Mathematik und Physik ZAMP* 21, no. 2 (1970): 187-195.

[12] Chapman, Thomas W., and Gerald L. Bauer. "Stagnation-point viscous flow of an incompressible fluid between porous plates with uniform blowing." *Applied Scientific Research* 31, no. 3 (1975): 223-239.

[13] Agarwal, R. S., and C. Dhanapal. "Stagnation point micropolar fluid flow between porous discs with uniform blowing." *International journal of engineering science* 26, no. 3 (1988): 293-300.

[14] Elcrat, Alan R. "On the radial flow of a viscous fluid between porous disks." *Archive for Rational Mechanics and Analysis*61, no. 1 (1976): 91-96.

[15] Bujurke, N. M., N. P. Pai, and P. K. Achar. "Semi-analytic approach to stagnation-point flow between porous plates with mass transfer." *Indian Journal of Pure and Applied Mathematics* 26 (1995): 373-390.

[16] Wang, C. Y. "Exact solutions of the steady-state Navier-Stokes equations." *Annual Review of Fluid Mechanics* 23, no. 1 (1991): 159-177.

[17] Wang, C. Y. "Similarity stagnation point solutions of the Navier–Stokes equations–review and extension." *European Journal of Mechanics-B/Fluids* 27, no. 6 (2008): 678-683.

[18] Mahapatra, T. Roy, and A. S. Gupta. "Magnetohydrodynamic stagnation-point flow towards a stretching sheet." *Acta Mechanica* 152, no. 1-4 (2001): 191-196.

[19] Beavers, Gordon S., and Daniel D. Joseph. "Boundary conditions at a naturally permeable wall." *Journal of fluid mechanics* 30, no. 1 (1967): 197-207.

[20] Nield, D. A. "The Beavers–Joseph boundary condition and related matters: a historical and critical note." *Transport in porous media* 78, no. 3 (2009): 537.

[21] Bhat, Ashwini, N. N. Katagi, and Sesappa A. Rai. "Analysis of Laminar Flow through a Porous Channel with Velocity Slip." *Malaysian Journal of Mathematical Sciences* 11, no. 3.

[22] Bhat, Ashwini, N. N. Katagi, and N. M. Bujurke. "Analysis of Laminar Flow in a Porous Pipe with Slip Velocity." *Journal of Mechanical Engineering Research and Developments* 40, no. 4 (2017): 1-11.

[23] Van Dyke, Milton. "Analysis and improvement of perturbation series." *The Quarterly Journal of Mechanics and Applied Mathematics* 27, no. 4 (1974): 423-450.

[24] Van Dyke, Milton. "Perturbation methods in fluid mechanics/Annotated edition." *NASA STI/Recon Technical Report A* 75 (1975).

[25] Dyke, M. Van. "Computer-extended series." *Annual Review of Fluid Mechanics* 16, no. 1 (1984): 287-309.

[26] Bujurke, Nagendrappa, Nagaraj N. Katagi, and V. B. Awati. "Analysis of Laminar flow in a channel with one porous bounding wall." *International Journal of Fluid Mechanics Research* 37, no. 3 (2010).

[27] Domb, Cyril, and M. F. Sykes. "On the susceptibility of a ferromagnetic above the Curie point." *Proc. R. Soc. Lond. A*240, no. 1221 (1957): 214-228.

[28] Liao, Shijun. *Beyond perturbation: introduction to the homotopy analysis method*. CRC press, 2003.

[29] Liao, Shijun. *Homotopy analysis method in nonlinear differential equations*. Beijing: Higher education press, 2012.

[30] Aziz, A., and Tsung Yen Na. "Perturbation methods in heat transfer." *Washington, DC, Hemisphere Publishing Corp., 1984, 212 p.* (1984).

[31] Bender, Carl M., and Steven A. Orszag. *Advanced mathematical methods for scientists and engineers I: Asymptotic methods and perturbation theory*. Springer Science & Business Media, 2013.

[32] Brady, J. F. "Flow development in a porous channel and tube." *The Physics of fluids* 27, no. 5 (1984): 1061-1067.

[33] Brady, J. F., and A. Acrivos. "Steady flow in a channel or tube with an accelerating surface velocity. An exact solution to the Navier—Stokes equations with reverse flow." *journal of Fluid Mechanics* 112 (1981): 127-150.

[34] Cox, Stephen M. "Analysis of steady flow in a channel with one porous wall, or with accelerating walls." *SIAM Journal on Applied Mathematics* 51, no. 2 (1991): 429-438.

[35] Liao, Sh J. "The proposed homotopy analysis technique for the solution of nonlinear problems." PhD diss., Ph. D. Thesis, Shanghai Jiao Tong University, 1992.

[36] Nayfeh. *Introduction to Perturbation Techniques.* John Wiley and Sons, New York, 1981.

[37] Robinson, W. A. "The existence of multiple solutions for the laminar flow in a uniformly porous channel with suction at both walls." *Journal of Engineering Mathematics* 10, no. 1 (1976): 23-40.

[38] Skalak, Francis M., and Chang Yi Wang. "On the nonunique solutions of laminar flow through a porous tube or channel." *SIAM Journal on Applied Mathematics* 34, no. 3 (1978): 535-544.

[39] Sparrow, E. M., G. S. Beavers, and L. Y. Hung. "Channel and tube flows with surface mass transfer and velocity slip." *The Physics of Fluids* 14, no. 7 (1971): 1312-1319.

[40] Terrill, R. M., and J. P. Cornish. "Radial flow of a viscous, incompressible fluid between two stationary, uniformly porous discs." *Zeitschrift für angewandte Mathematik und Physik ZAMP* 24, no. 5 (1973): 676-688.

[41] Wah, Thein. "Laminar flow in a uniformly porous channel." *The Aeronautical Quarterly* 15, no. 3 (1964): 299-310.

Appendix

Table 1: Values of θ, θ' and D_p at various Reynolds number for $\phi = 0$.

z	R=0.1		R=1		R=10		R=100		R=1000		R=10000		R=100000	
	−q	−q'	−q	−q'	−q	−q'	−q	−q'	−q	−q'	−q	−q'	−q	−q'
0.0	0.00000	1.50338	0.00000	1.53258	0.00000	1.70672	0.00000	1.89268	0.00000	1.96497	0.00000	1.98889	0.00000	1.99669
0.1	0.14983	1.48817	0.15269	1.51549	0.16955	1.67288	0.18594	1.79784	0.18958	1.80091	0.18996	1.80014	0.19000	1.80001
0.2	0.29662	1.44257	0.30197	1.46449	0.33250	1.57691	0.35651	1.60876	0.35967	1.59975	0.35997	1.60020	0.36000	1.60010
0.3	0.43733	1.36665	0.44448	1.38034	0.48326	1.43217	0.50732	1.40768	0.50975	1.40012	0.50997	1.40012	0.51000	1.40001
0.4	0.56894	1.26051	0.57697	1.26425	0.61936	1.25417	0.63804	1.20658	0.63982	1.20065	0.63998	1.20015	0.64000	1.20001
0.5	0.68844	1.12432	0.69632	1.11780	0.73360	1.05809	0.74864	0.99947	0.74987	1.00053	0.74999	1.00005	0.75000	1.00001
0.6	0.79281	0.95820	0.79958	0.94290	0.81219	0.85170	0.83913	0.80440	0.83992	0.80040	0.83999	0.80000	0.84000	0.80000
0.7	0.87910	0.76252	0.88401	0.74151	0.90652	0.64065	0.90951	0.60330	0.90995	0.60037	0.91000	0.60004	0.91000	0.60004
0.8	0.94434	0.53739	0.94741	0.51588	0.97926	0.42772	0.95978	0.40221	0.95998	0.40021	0.96000	0.40002	0.96000	0.40002
0.9	0.98560	0.28313	0.98644	0.26799	0.98930	0.21394	0.98995	0.20113	0.98999	0.20012	0.99000	0.20001	0.99000	0.20001
1.0	1.00000	0.00000	1.00000	0.00000	1.00000	0.00000	1.00000	0.00000	1.00000	0.00000	1.00000	0.00000	1.00000	0.00000
Dp	63.09800		9.19263		4.28365		4.02186		4.00200		4.00024		4.00000	

Table 2: Values of θ, θ' and D_p at various Reynolds number for $\phi = 0.1$.

z	R=0.1		R=1		R=10		R=100		R=1000		R=10000		R=100000	
	−q	−q'	−q	−q'	−q	−q'	−q	−q'	−q	−q'	−q	−q'	−q	−q'
0.0	0.00000	1.38778	0.00000	1.41525	0.00000	1.61832	0.00000	1.87774	0.00000	1.89683	0.00000	1.90396	0.00000	2.00126
0.1	0.14983	1.37607	0.15269	1.40186	0.16955	1.54860	0.18643	1.79871	0.18721	1.87223	0.19003	1.89003	0.19000	1.97819
0.2	0.29662	1.34096	0.30197	1.36239	0.33250	1.50813	0.36036	1.77256	0.37014	1.85270	0.37994	1.86238	0.38200	1.86336
0.3	0.43733	1.28249	0.44448	1.29684	0.48326	1.41534	0.51912	1.61563	0.52794	1.67828	0.53007	1.68588	0.53100	1.68666
0.4	0.56894	1.20076	0.57697	1.20765	0.61936	1.28119	0.63870	1.29610	0.64808	1.29841	0.64941	1.30192	0.65002	1.31897
0.5	0.68844	1.09584	0.69632	1.09255	0.73360	1.05024	0.75046	1.02223	0.75944	1.02300	0.76141	1.15300	0.76100	1.15659
0.6	0.79281	0.96791	0.79958	0.97561	0.81219	0.98805	0.83494	0.98771	0.84659	0.98935	0.84951	0.99497	0.85002	1.00559
0.7	0.87910	0.81923	0.88401	0.81923	0.90652	0.81923	0.92276	0.81923	0.93309	0.81923	0.93010	0.81923	0.93002	0.81923
0.8	0.94434	0.64360	0.94741	0.62210	0.94926	0.49351	0.95520	0.31813	0.96296	0.27555	0.96107	0.27068	0.96003	0.27019
0.9	0.98560	0.44761	0.98644	0.42790	0.98930	0.32315	0.98685	0.20892	0.98654	0.18506	0.99968	0.18241	0.99014	0.18215
1.0	1.00000	0.22934	1.00000	0.21779	1.00000	0.17705	1.00000	0.14861	1.00000	0.03702	1.00000	0.00423	1.00000	0.00043
Dp	48.76843		7.32153		4.62626		3.55640		3.55252		3.55008		3.55000	

Table 3: Values of θ, θ' and D_p at various Reynolds number for $\phi = 0.5$.

z	R=0.1		R=1		R=10		R=100		R=1000		R=10000		R=100000	
	−q	−q'	−q	−q'	−q	−q'	−q	−q'	−q	−q'	−q	−q'	−q	−q'
0.0	0.00000	1.20203	0.00000	1.21972	0.00000	1.37390	0.00000	1.46613	0.00000	1.65482	0.00000	1.65518	0.00000	1.60045
0.1	0.12000	1.19593	0.12174	1.21277	0.13243	1.31704	0.18024	1.39115	0.18977	1.40967	0.18558	1.41199	0.18900	1.41179
0.2	0.23878	1.16422	0.24209	1.18523	0.26066	1.29770	0.26666	1.31058	0.27242	1.32099	0.28194	1.37565	0.28452	1.44098
0.3	0.35512	1.14721	0.35968	1.15753	0.38575	1.20593	0.39629	1.22787	0.40932	1.23657	0.40847	1.24043	0.40001	1.25800
0.4	0.46782	1.10464	0.47316	1.10992	0.50275	1.12422	0.51677	1.10066	0.51983	1.02352	0.52169	1.00362	0.52200	1.00037
0.5	0.57565	1.05000	0.58124	1.04964	0.60856	1.03185	0.60956	1.13994	0.61172	1.01388	0.62587	1.00282	0.62106	1.00220
0.6	0.67742	0.98334	0.68269	0.97745	0.70859	0.92218	0.71647	0.58910	0.72582	0.12774	0.74009	0.01446	0.74029	0.00147
0.7	0.77192	0.90474	0.77633	0.89378	0.79795	0.83221	0.80296	0.79870	0.81448	0.78782	0.80816	0.78615	0.80030	0.78597
0.8	0.85797	0.81429	0.86109	0.79973	0.87498	0.72901	0.87904	0.59023	0.87793	0.17378	0.90169	0.02147	0.90040	0.00220
0.9	0.93439	0.71209	0.93595	0.69601	0.94490	0.62515	0.95604	0.58251	0.95858	0.28550	0.95887	0.04511	0.95890	0.00479
1.0	1.00000	0.59823	1.00000	0.58347	1.00000	0.60218	1.00000	0.10657	1.00000	0.01316	1.00000	0.00135	1.00000	0.00000
Dp	25.47242		3.94584		3.32353		3.32112		3.32005		3.32001		3.32000	

Appendix

Table 1

Values of θ, θ' and D_p at various Reynolds number for $\phi = 0$.

	R=0.1		**R=1**		**R=10**		**R=100**		**R=1000**		**R=10000**		**R=100000**	
z	**−q**	**−q'**	**−q**	**−q'**	**−q**	**−q'**	**−q**	**−q'**	**−q**	**−q'**	**−q**	**−q'**	**−q**	**−q'**
0.0	0.00000	1.50338	0.00000	1.53258	0.00000	1.70672	0.00000	1.89268	0.00000	1.96497	0.00000	1.98889	0.00000	1.99669
0.1	0.14983	1.48817	0.15269	1.51549	0.16955	1.67288	0.18594	1.79784	0.18958	1.80091	0.18996	1.80014	0.19000	1.80001
0.2	0.29662	1.44257	0.30197	1.46449	0.33250	1.57691	0.35651	1.60876	0.35967	1.59975	0.35997	1.60020	0.36000	1.60010
0.3	0.43733	1.36665	0.44448	1.38034	0.48326	1.43217	0.50732	1.40768	0.50975	1.40012	0.50997	1.40012	0.51000	1.40001
0.4	0.56894	1.26051	0.57697	1.26425	0.61936	1.25417	0.63804	1.20658	0.63982	1.20065	0.63998	1.20015	0.64000	1.20001
0.5	0.68844	1.12432	0.69632	1.11780	0.73360	1.05809	0.74864	0.99947	0.74987	1.00053	0.74999	1.00005	0.75000	1.00001
0.6	0.79281	0.95820	0.79958	0.94290	0.81219	0.85170	0.83913	0.80440	0.83992	0.80040	0.83999	0.80000	0.84000	0.80000
0.7	0.87910	0.76252	0.88401	0.74151	0.90652	0.64065	0.90951	0.60330	0.90995	0.60037	0.91000	0.60004	0.91000	0.60004
0.8	0.94434	0.53739	0.94741	0.51588	0.97926	0.42772	0.95978	0.40221	0.95998	0.40021	0.96000	0.40002	0.96000	0.40002
0.9	0.98560	0.28313	0.98644	0.26799	0.98930	0.21394	0.98995	0.20113	0.98999	0.20012	0.99000	0.20001	0.99000	0.20001
1.0	1.00000	0.00000	1.00000	0.00000	1.00000	0.00000	1.00000	0.00000	1.00000	0.00000	1.00000	0.00000	1.00000	0.00000
Dp	63.09800		9.19263		4.28365		4.02186		4.00200		4.00024		4.00000	

Table 2

Values of θ, θ' and D_p at various Reynolds number for $\phi = 0.1$.

z	R=0.1		R=1		R=10		R=100		R=1000		R=10000		R=100000	
	−q	−q'	−q	−q'	−q	−q'	−q	−q'	−q	−q'	−q	−q'	−q	−q'
0.0	0.00000	1.38778	0.00000	1.41525	0.00000	1.61832	0.00000	1.87774	0.00000	1.89683	0.00000	1.90396	0.00000	2.00126
0.1	0.14983	1.37607	0.15269	1.40186	0.16955	1.54860	0.18643	1.79871	0.18721	1.87223	0.19003	1.89003	0.19000	1.97819
0.2	0.29662	1.34096	0.30197	1.36239	0.33250	1.50813	0.36036	1.77256	0.37014	1.85270	0.37994	1.86238	0.38200	1.86336
0.3	0.43733	1.28249	0.44448	1.29684	0.48326	1.41534	0.51912	1.61563	0.52794	1.67828	0.53007	1.68588	0.53100	1.68666
0.4	0.56894	1.20076	0.57697	1.20765	0.61936	1.28119	0.63870	1.29610	0.64808	1.29841	0.64941	1.30192	0.65002	1.31897
0.5	0.68844	1.09584	0.69632	1.09255	0.73360	1.05024	0.75046	1.02223	0.75944	1.02300	0.76141	1.15300	0.76100	1.15659
0.6	0.79281	0.96791	0.79958	0.97561	0.81219	0.98805	0.83494	0.98771	0.84659	0.98935	0.84951	0.99497	0.85002	1.00559
0.7	0.87910	0.81923	0.88401	0.81923	0.90652	0.81923	0.92276	0.81923	0.93309	0.81923	0.93010	0.81923	0.93002	0.81923
0.8	0.94434	0.64360	0.94741	0.62210	0.94926	0.49351	0.95520	0.31813	0.96296	0.27555	0.96107	0.27068	0.96003	0.27019
0.9	0.98560	0.44761	0.98644	0.42790	0.98930	0.32315	0.98685	0.20892	0.98654	0.18506	0.99968	0.18241	0.99014	0.18215
1.0	1.00000	0.22934	1.00000	0.21779	1.00000	0.17705	1.00000	0.14861	1.00000	0.03702	1.00000	0.00423	1.00000	0.00043
Dp	48.76843		7.32153		4.62626		3.55640		3.55252		3.55008		3.55000	

Table 3

Values of θ, θ' and D_p at various Reynolds number for $\phi = 0.5$.

z	R=0.1		R=1		R=10		R=100		R=1000		R=10000		R=100000	
	−q	−q'	−q	−q'	−q	−q'	−q	−q'	−q	−q'	−q	−q'	−q	−q'
0.0	0.00000	1.20203	0.00000	1.21972	0.00000	1.37390	0.00000	1.46613	0.00000	1.65482	0.00000	1.65518	0.00000	1.60045
0.1	0.12000	1.19593	0.12174	1.21277	0.13243	1.31704	0.18024	1.39115	0.18977	1.40967	0.18558	1.41199	0.18900	1.41179
0.2	0.23878	1.16422	0.24209	1.18523	0.26066	1.29770	0.26666	1.31058	0.27242	1.32099	0.28194	1.37565	0.28452	1.44098
0.3	0.35512	1.14721	0.35968	1.15753	0.38575	1.20593	0.39629	1.22787	0.40932	1.23657	0.40847	1.24043	0.40001	1.25800
0.4	0.46782	1.10464	0.47316	1.10992	0.50275	1.12422	0.51677	1.10066	0.51983	1.02352	0.52169	1.00362	0.52200	1.00037
0.5	0.57565	1.05000	0.58124	1.04964	0.60856	1.03185	0.60956	1.13994	0.61172	1.01388	0.62587	1.00282	0.62106	1.00220
0.6	0.67742	0.98334	0.68269	0.97745	0.70859	0.92218	0.71647	0.58910	0.72582	0.12774	0.74009	0.01446	0.74029	0.00147
0.7	0.77192	0.90474	0.77633	0.89378	0.79795	0.83221	0.80296	0.79870	0.81448	0.78782	0.80816	0.78615	0.80030	0.78597
0.8	0.85797	0.81429	0.86109	0.79973	0.87498	0.72901	0.87904	0.59023	0.87793	0.17378	0.90169	0.02147	0.90040	0.00220
0.9	0.93439	0.71209	0.93595	0.69601	0.94490	0.62515	0.95604	0.58251	0.95858	0.28550	0.95887	0.04511	0.95890	0.00479
1.0	1.00000	0.59823	1.00000	0.58347	1.00000	0.60218	1.00000	0.10657	1.00000	0.01316	1.00000	0.00135	1.00000	0.00000
Dp	25.47242		3.94584		3.32353		3.32112		3.32005		3.32001		3.32000	